Computational Mechanics 24 (1999) 41–51 © Springer-Verlag 1999

Determination of spurious eigenvalues and multiplicities of true eigenvalues using the real-part dual BEM

J. T. Chen, C. X. Huang, K. H. Chen

Abstract The complex-valued dual BEM has been employed by Chen and Chen (1998) to solve the acoustic modes of a cavity with or without a thin partition. A novel method using only the real part of the complex-valued dual BEM was found by Chen (1998) to be equivalent to the dual MRM. However, spurious eigenvalues occur. In this paper, we propose the singular value decomposition technique to filter out spurious eigenvalues and to determine the multiplicity of true eigenvalues by combining the real-part dual equations. Also, the role of the real-part dual BEM for problems with a degenerate boundary is examined. Four examples, including a square cavity with multiple eigenvalues, a rectangular cavity, a rectangular cavity with a zero thickness partition and a rectangular cavity with a partition with finite thickness, are presented to demonstrate the validity of the proposed method. Also, the analytical solution if available, the FEM results obtained by Petyt et al. and obtained using ABAQUS and the experimental measurements are compared with those of the proposed method, and it is found that agreement between them is very good.

1 Introduction

The complex-valued dual BEM has been used by Chen and Chen (1998) to solve the Helmholtz problems with a degenerate boundary. To avoid complex-valued computation, the multiple reciprocity method (MRM) can be employed (Nowak and Neves, 1994). A novel method using only the real part of the complex-valued dual BEM was found by Chen (1998) to be equivalent to the dual MRM if the zeroth-order fundamental solution is properly chosen. This method has been termed the simplified technique by De Mey (1977), and only the first eigenvalue is calculated. Nevertheless, the real-valued formulation (MRM or real-part BEM) results in spurious solutions. The analytical formulation for the one dimensional case was studied by Chen and Wong (1997) using the MRM. Numerical experiments in spurious eigenvalues were performed for the two dimensional case by Chen and Wong (1998) using the MRM. For the real-part BEM, Liou, Chen and Chen (1999) also found the spurious solutions numerically for the two- dimensional Helmholtz equation. One advantage of using only the real-part kernels is that only real-valued computation is considered instead of the complex-valued computation used in the complex-valued BEM. Another benefit is that the lengthy derivation needed for the MRM can be avoided. However, some drawbacks of the real-valued formulation for the Helmholtz equation have been found by Chen and Wong (1997) to occur with spurious eigenvalues and failure was found by Chen and Wong (1998) when it was applied to problems with a degenerate boundary. For the spurious solution, it occurs in the MRM or the real-part BEM due to the loss of the imaginary part, which was investigated by Yeih et al. (1997). The loss of constraints in the imaginary part makes the eigensolution space large and results in spurious eigenvalues. The relations among the MRM, the real-part BEM and the complex-valued BEM were discussed in a keynote lecture by Chen (1998). The framework of the real-part "dual" BEM was constructed so as to filter out spurious eigenvalues and at the same time to avoid - nonunique solutions for problems with a degenerate boundary. By employing the dual MRM (Chen and Wong, 1998) or the real-part dual BEM (Liou, Chen and Chen, 1999), spurious eigenvalues can be filtered out by checking the residue between the singular and hypersingular equations. The residue method was successfully employed by Chen and Wong (1997), and Chen and Wong (1998), respectively, to filter out spurious solutions for one and two-dimensional problems. However, the boundary modes (including the true and spurious modes) should be determined in advance before finding the residue. In some cases, e.g., double roots (Chen, Chen and Chyuan, 1999) and a null matrix with rank deficiency (Chen and Wong, 1997), it is not straightforward to determine the boundary modes. Finding a more efficient method to distinguish whether an eigenvalue is true or not is not trivial, and this was the main motivation of the present study. The SVD technique was employed to filter out spurious modes for a rod (Yeih, Chang, Chang and Chen, 1999), and an Euler-Bernouli beam (Yeih, Chen and Chang, 1999) more efficiently than can be done using the residue method presented by Chen and Wong (1998). Also, the spurious eigenvalues depend on the interface position of the subdomain and can be separated by adjusting the connections among subdomains as shown in Chang, Yeih and Chen (1999). However, all the applications using SVD or the

J.T. Chen ( ), C.X. Huang, K.H. Chen
Department of Harbor and River Engineering,
National Taiwan Ocean University, Keelung, Taiwan
E-mail: B0209@ntou66.ntou.edu.tw

Financial support from the National Science Council under Grant No. NSC-88-2211-E-019-005 for National Taiwan Ocean University is gratefully acknowledged.

domain partition technique have focused on one-dimensional examples. We will extend them to two-dimensional cases. After finding the true eigenvalue, determining its multiplicity is also our concern. For the problem with a degenerate boundary, the dual formulation is the key step in solving the problem of the nonuniqueness of the solution (Chen and Hong, 1992; Chen and Chen, 1998). A detailed review article including 250 references written by Chen and Hong (1999) can be referred to. In another words, the real-part dual BEM in conjunction with SVD can be used to solve the problems with spurious eigenvalues and a degenerate boundary at the same time. Both roles of the dual formulation, one for filtering out the spurious solution and the other for the degenerate boundary problem, will be examined.

In this paper, we employ the real-part dual BEM to solve the acoustic problems of a cavity with or without a thin partition, and with or without multiple eigenvalues. After assembling the dual equations, a singular value decomposition (SVD) technique is extended to filter out spurious eigenvalues for two-dimensional cavities more efficiently than can be done using the residue method described by Chen and Wong (1998). Also, the multiplicities of the true eigenvalues are determined using the same method. The roles of the SVD technique in the real-part dual BEM are examined. Four examples, including a square cavity, a rectangular cavity with a finite-thickness partition, and a rectangular cavity with zero thickness and no partition, are employed to check the validity of the proposed method. Finally, the solutions are compared with the exact solutions, experimental data and FEM results obtained using MSC/ABAQUS (1996) and obtained by Petyt et al. (1996, 1997) to check the validity of the present formulation.

2 Dual integral formulation of the real-part dual BEM for a two-dimensional acoustic cavity with or without a thin partition

The governing equation for an acoustic cavity is the Helmholtz equation:

$$(\nabla^2 + k^2)u(x) = 0, \quad x \in D \ ,$$

where ∇^2 is the Laplacian operator, D is the domain of the cavity and k is the wave number, which is the frequency over the speed of sound. The boundary conditions can be either of the Neumann or Dirichlet type.

Based on the complex-valued dual formulation derived by Chen and Chen (1998), the dual equations for the boundary points are

$$\pi u(x) = \text{C.P.V.} \int_B T_c(s,x)u(s)\mathrm{d}B(s) - \text{R.P.V.} \int_B U_c(s,x)t(s)\mathrm{d}B(s), \quad x \in B \tag{1}$$

$$\pi t(x) = \text{H.P.V.} \int_B M_c(s,x)u(s)\mathrm{d}B(s) - \text{C.P.V.} \int_B L_c(s,x)t(s)\mathrm{d}B(s), \quad x \in B \ , \tag{2}$$

where C.P.V., R.P.V. and H.P.V. denote the Cauchy principal value, the Riemann principal value and the Hadamard principal value, $t(s) = \partial u(s)/\partial n_s$; B denotes the boundary enclosing D; the four kernels, $U_c(s,x), T_c(s,x), L_c(s,x)$, and $M_c(s,x)$ are complex, and their explicit forms can be found in Chen and Chen (1998). It is well known that MRM is no more than the real-part formulation of the complex-valued BEM (Kamiya et al., 1996; Yeih et al., 1997). This indicates that the real-part kernels of the complex-valued BEM can be adopted for the Helmholtz equation free of the lengthy derivation of MRM. Therefore, we have the real-part kernels as follows:

$$U(s,x) = \text{Real}\{U_c(s,x)\} = \frac{\pi Y_0^{(1)}(kr)}{2} \ , \tag{3}$$

$$T(s,x) = \text{Real}\{T_c(s,x)\} = \frac{k\pi}{2} Y_1^{(1)}(kr)\frac{y_i n_i}{r} \ , \tag{4}$$

$$L(s,x) = \text{Real}\{L_c(s,x)\} = \frac{-k\pi}{2} Y_1^{(1)}(kr)\frac{y_i \bar{n}_i}{r} \ , \tag{5}$$

$$M(s,x) = \text{Real}\{M_c(s,x)\} = \frac{k\pi}{2}\left\{-k\frac{Y_2^{(1)}(kr)}{r^2} y_i y_j n_i \bar{n}_j + \frac{Y_1^{(1)}(kr)}{r} n_i \bar{n}_i\right\} \ , \tag{6}$$

where $Y_n^{(1)}(kr)$ denotes the imaginary part of the nth order of the Hankel function $(H_n^{(1)}(kr))$: r is the distance between the source point and field point; n_i is the ith component of the normal vector at s; $\bar{n}_i$ is the ith component of normal vector at x; $y_i \equiv s_i - x_i$. The U kernel in Eq. (3) can be expanded into series form for comparison with that of the MRM derived by Chen (1998) as shown below:

$$U(s,x) = \sum_{j=0}^{\infty} (-k^2)^j U_j(s,x) \ , \tag{7}$$

where

$$U_0(s,x) = \ln(r) + \gamma + \ln\left(\frac{k}{2}\right), \quad j = 0 \ , \tag{8}$$

$$U_j(s,x) = 4F_j(\ln(r) - S_j) + F_j\left(\gamma + \ln\left(\frac{k}{2}\right)\right), \quad j = 1,2,3,\ldots \ , \tag{9}$$

$$\gamma = \lim_{j\to\infty}\left(\sum_{l=1}^{j}\frac{1}{l} - \ln(j)\right) \ , \tag{10}$$

$$F_j = \frac{r^{2j}}{(j!)^2 4^j} \ , \tag{11}$$

$$S_j = \sum_{l=1}^{j}\frac{1}{l} \ , \tag{12}$$

in which γ is an Euler constant. It is interesting to find that the series form for the real-part closed-form kernels is very similar to that derived from MRM. The major difference between them is a real constant, $\gamma + \ln(k/2)$, in the zeroth order fundamental solution. All four kernels satisfy the dual properties as follows: $U(s,x) = U(x,s)$, $T(s,x) = L(x,s)$ and $M(s,x) = M(x,s)$. In this paper, we term the

real-part UT singular formulation in Eq. (1) the "*UT* method" while the real-part LM hypersingular formulation in Eq. (2) is called the "*LM* method".

3 Discretization of the real-part dual boundary integral equations

By employing the constant element scheme, Eqs. (1) and (2) can be discretized into the following linear algebraic equations:

$$[\mathbf{T}(k)-\pi\mathbf{I}]\{\mathbf{u}\}=[\mathbf{U}(k)]\{\mathbf{t}\}\ , \tag{13}$$

$$[\mathbf{M}(k)]\{\mathbf{u}\}=[\mathbf{L}(k)+\pi\mathbf{I}]\{\mathbf{t}\}\ , \tag{14}$$

where $\{\mathbf{u}\}$ and $\{\mathbf{t}\}$ are the column vectors for the boundary data, $\mathbf{I}$ is a unit matrix, and $[\mathbf{U}(k)]$, $[\mathbf{T}(k)]$, $[\mathbf{L}(k)]$ and $[\mathbf{M}(k)]$ are the influence matrices resulting from the U, T, L and M kernels.

(1) U kernel:

For the regular integral, we have

$$U_{ij}=\frac{\pi}{2}\int_{-0.5l}^{0.5l}Y_0^{(1)}\left(k\sqrt{(x_r-s)^2+y_r^2}\right)\mathrm{d}s,\quad (i\neq j)\ , \tag{15}$$

where x_r and y_r are coordinates after translation and rotation following the symbols used by Chen and Hong (1992).

For the weakly singular integral, we regularize by means of partial integration as follows:

$$\begin{aligned}U_{ii}&=\frac{\pi}{2}\lim_{\epsilon\to 0}\int_{-0.5l}^{0.5l}Y_0^{(1)}\left(k\sqrt{s^2+\epsilon^2}\right)\mathrm{d}s\\&=\frac{\pi}{2}\left\{Y_0^{(1)}\left(\frac{kl}{2}\right)l+k\int_{-0.5l}^{0.5l}\left\{Y_1^{(1)}(k|s|)|s|\,\mathrm{d}s\right\},\right.\\&\quad (i\text{ no sum})\ .\end{aligned} \tag{16}$$

(2) T kernel:

For the regular integral, we have

$$\begin{aligned}T_{ij}=&-\frac{\pi k}{2}\int_{-0.5l}^{0.5l}Y_1^{(1)}\left(k\sqrt{(x_r-s)^2+y_r^2}\right)\\&\times\frac{y_r}{\sqrt{(x_r-s)^2+y_r^2}}\,\mathrm{d}s,\quad (i\neq j)\ .\end{aligned} \tag{17}$$

For the strongly singular integral, we have

$$\begin{aligned}T_{ii}&=-\frac{\pi k}{2}\lim_{\epsilon\to 0}\int_{-0.5l}^{0.5l}Y_1^{(1)}\left(k\sqrt{s^2+\epsilon^2}\right)\frac{\epsilon}{\sqrt{s^2+\epsilon^2}}\,\mathrm{d}s\\&=\pi,\quad (i\text{ no sum})\ .\end{aligned} \tag{18}$$

(3) L kernel:

For the regular integral, we have

$$\begin{aligned}L_{ij}=&-\frac{\pi k}{2}\int_{-0.5l}^{0.5l}Y_1^{(1)}\left(k\sqrt{(x_r-s)^2+y_r^2}\right)\\&\times\frac{(x_r-s)\sin(\phi-\theta)-y_r\cos(\phi-\theta)}{\sqrt{(x_r-s)^2+y_r^2}}\mathrm{d}s,\quad (i\neq j)\ ,\end{aligned} \tag{19}$$

where ϕ and θ are the associated angles for x and s, respectively, and were defined by Chen and Hong (1992).

For the strongly singular integral, we have

$$\begin{aligned}L_{ii}&=-\frac{\pi k}{2}\lim_{\epsilon\to 0}\int_{-0.5l}^{0.5l}Y_1^{(1)}\left(k\sqrt{s^2+\epsilon^2}\right)\frac{-\epsilon}{\sqrt{s^2+\epsilon^2}}\,\mathrm{d}s\\&=\lim_{\epsilon\to 0}\frac{\pi k}{2}\int_{-\sqrt[4]{\epsilon}}^{\sqrt[4]{\epsilon}}\frac{(-2)}{\pi k\sqrt{s^2+\epsilon^2}}\frac{\epsilon}{\sqrt{s^2+\epsilon^2}}\,\mathrm{d}s\\&=-\pi,\quad (i\text{ no sum})\ .\end{aligned} \tag{20}$$

(4) M kernel:

For the regular integral, we have

$$\begin{aligned}M_{ij}=&\frac{\pi k}{2}\int_{-0.5l}^{0.5l}-k\frac{Y_2^{(1)}\left(k\sqrt{(x_r-s)^2+y_r^2}\right)}{(x_r-s)^2+y_r^2}(-y_r)\\&\times\{(x_r-s)\sin(\phi-\theta)-y_r\cos(\phi-\theta)\}\\&+\frac{Y_1^{(1)}\left(k\sqrt{(x_r-s)^2+y_r^2}\right)}{\sqrt{(x_r-s)^2+y_r^2}}\cos(\phi-\theta)\mathrm{d}s,\quad (i\neq j).\end{aligned} \tag{21}$$

For the hypersingular integral, we regularize by means of partial integration as follows:

$$\begin{aligned}M_{ii}=&\frac{\pi k}{2}\lim_{\epsilon\to 0}\int_{-0.5l}^{0.5l}-k\frac{Y_2^{(1)}\left(k\sqrt{s^2+\epsilon^2}\right)}{s^2+\epsilon^2}(-\epsilon)(-\epsilon)\\&+\frac{Y_1^{(1)}\left(k\sqrt{-s^2+\epsilon^2}\right)}{\sqrt{s^2+\epsilon^2}}\mathrm{d}s\\=&\frac{\pi k}{2}\left\{-2Y_1^{(1)}\left(\frac{kl}{2}\right)+k\left[Y_0^{(1)}\left(\frac{kl}{2}\right)\right.\right.\\&\left.\left.+k\int_{-0.5l}^{0.5l}Y_1^{(1)}(k|s|)|s|\,\mathrm{d}s\right]\right\},\ (i\text{ no sum})\ .\end{aligned} \tag{22}$$

All the above regular integrals can be calculated by using the Gaussian quadrature rule.

4 Detection of spurious eigenvalues and determination of the multiplicities of true eigenvalues using the singular value decomposition technique for the real-part dual BEM

According to Eqs. (13) and (14), we can obtain the eigenvalues independently for the problem without degenerate boundaries. However, spurious eigenvalues will be imbedded if the *UT* Eq. (13) or *LM* equation (14) is used alone. As mentioned by Kamiya et al. (1996), the equation derived using MRM is no more than a real part of the complex-valued formulation. Since the series form of the real-part BEM only differs from the conventional MRM in the zeroth order fundamental solution by a constant term, the loss of the imaginary part in either the real-part BEM or MRM results in spurious eigenvalues. Nevertheless, their spurious eigenvalues occur at different positions. Yeih et al. (1997) extended the general proof for any dimensional problem and demonstrated it using a one-

dimensional case. The imaginary part in the complex-valued formulation is not present in the real-part BEM or the MRM, and the number of constraints for the eigenequation is insufficient. Therefore, the solution space for the eigensystem is large, and spurious eigenvalues are present. These findings can explain why spurious eigenvalues occur when the real-part BEM or MRM is used when either Eq. (13) or (14) is employed alone; i.e. the mechanism of the spurious eigenvalues can be understood in this way. The residue technique used to filter out spurious eigenvalues (Chen and Wong, 1998) is summarized as below.

Since only the real part is of concern in the real-part BEM or MRM, an approach to obtaining enough constraints for the eigenequation was obtained in the dual formulation through differentiation with respect to the real-part BEM or the conventional MRM. This method results in the real-part dual BEM (Liou, Chen and Chen, 1999) and the dual MRM (Chen and Wong, 1998) with hypersingular integral equations. For simplicity, we will deal with the Neumann problem. Therefore, Eqs. (13) and (14) reduce to

$$[\bar{\mathbf{T}}(k)]\{\mathbf{u}\} = \{0\} \ , \tag{23}$$

$$[\mathbf{M}(k)]\{\mathbf{u}\} = \{0\} \ , \tag{24}$$

where $[\bar{\mathbf{T}}(k)]$ differs from $[\mathbf{T}(k)]$ by a jump term. In the residue method (Chen and Wong, 1998; Liou, Chen and Chen, 1999), an approach used to detect spurious eigenvalues is to use the criterion of the residue to satisfy Eq. (13) (or Eq. (14)) when substituting the boundary modes obtained from Eq. (14) (or Eq. (13)) for the characteristic wave number, k. The spurious boundary modes obtained from Eq. (13) will not satisfy Eq. (14). Also, the spurious boundary modes obtained from Eq. (14) will not satisfy Eq. (13) in controversa. Therefore, two residual norms can be defined as follows:

$$\epsilon_T = [\bar{\mathbf{T}}(k_M)]\{u_M\} \ , \tag{25}$$

where $\{u_M\}$ is the boundary mode obtained from $[\mathbf{M}(k_M)]\{u_M\} = \{0\}$; or

$$\epsilon_M = [\mathbf{M}(k_T)]\{u_T\} \ , \tag{26}$$

where $\{u_T\}$ is the boundary mode which satisfies $[\bar{\mathbf{T}}(k_T)]\{u_T\} = 0$; ϵ_T and ϵ_M are the residue norms obtained by Eqs. (25) and (26), respectively; and k_M and k_T are the possible (true or spurious) eigenvalues obtained by Eqs. (23) and (24), respectively. By setting an appropriate value of the threshold, we can determine whether the eigenvalue is true or spurious. To double check, the acoustic modes can be examined based on the distribution of nodal lines and orthogonal properties after the possible true eigenvalues are determined.

It is noteworthy that the above technique needs to find the spurious boundary modes first from one equation (either the *UT* or *LM* equation) in the eigenvalue-searching stage and then substitute it into another eigenequation (either the *LM* or *UT* equation) to check the residuals. Now, we will present a more efficient way to filter out spurious eigenvalues which can avoid first determining the spurious boundary mode.

The eigenequations obtained by the *UT* and *LM* equations in Eqs. (23) and (24) can be rewritten as

$$[\bar{\mathbf{T}}(k)]_{N\times N}\{\mathbf{u}\}_{N\times 1} = \{0\} \ , \tag{27}$$

$$[\mathbf{M}(k)]_{N\times N}\{\mathbf{u}\}_{N\times 1} = \{0\} \ . \tag{28}$$

For problems with a degenerate boundary, we do the following. We first denote the normal boundary by S and the degenerate boundaries by C^+ and C^-, where C^+ and C^- are two surfaces on the degenerate boundary, which coincide with each other mathematically.

This means that $B = S + C^+ + C^-$. The *UT* method, which can be combined with the additional constraint *LM* equations by collocating the points on the degenerate boundary, has the eigenequation

$$\begin{bmatrix} \bar{T}_{i_S j_S} & \bar{T}_{i_S j_{C^+}} & \bar{T}_{i_S j_{C^-}} \\ \bar{T}_{i_{C^+} j_S} & \bar{T}_{i_{C^+} j_{C^+}} & \bar{T}_{i_{C^+} j_{C^-}} \\ M_{i_{C^+} j_S} & M_{i_{C^+} j_{C^+}} & M_{i_{C^+} j_{C^-}} \end{bmatrix} \begin{Bmatrix} u_{j_S} \\ u_{j_{C^+}} \\ u_{j_{C^-}} \end{Bmatrix} = \{0\} \ , \tag{29}$$

where the dependent rows in the $[\bar{\mathbf{T}}]$ matrix are replaced with rows obtained from the $[\mathbf{M}]$ matrix: i_S and i_{C^+} denote the collocation points on the S and C^+ boundaries, respectively; j_S and j_{C^+} denote the element ID on the S and C^+ boundaries, respectively.

In a similar way, the *LM* method, when combined with the additional constraint *UT* equations by collocating the degenerate boundary point, has the eigenequation

$$\begin{bmatrix} M_{i_S j_S} & M_{i_S j_{C^+}} & M_{i_S j_{C^-}} \\ \bar{T}_{i_{C^+} j_S} & \bar{T}_{i_{C^+} j_{C^+}} & \bar{T}_{i_{C^+} j_{C^-}} \\ M_{i_{C^+} j_S} & M_{i_{C^+} j_{C^+}} & M_{i_{C^+} j_{C^-}} \end{bmatrix} \begin{Bmatrix} u_{j_S} \\ u_{j_{C^+}} \\ u_{j_{C^-}} \end{Bmatrix} = \{0\} \ , \tag{30}$$

where the dependent rows in the $[\mathbf{M}]$ matrix are replaced with rows obtained from the $[\bar{\mathbf{T}}]$ matrix. To solve for the eigenequation, a direct search method has been employed to find the eigensolutions according to Eqs. (23) and (24). It is found that Eq. (13) or (14) can independently determine the possible eigenvalues (true and spurious) by using the direct-search method.

To distinguish spurious eigenvalues using the SVD technique, we can merge the two matrices in Eqs. (13) and (14) (or Eqs. (29) and (30) for the degenerate case) together to obtain

$$[\mathbf{C}(k)]_{2N\times N}\{\mathbf{u}\}_{N\times 1} = \{0\} \ , \tag{31}$$

where the $[\mathbf{C}(k)]$ matrix is derived from the $[\bar{\mathbf{T}}]$ and $[\mathbf{M}]$ matrices as follows:

$$[\mathbf{C}(k)]_{2N\times N} = \begin{bmatrix} \bar{\mathbf{T}}(k) \\ \mathbf{M}(k) \end{bmatrix} \ . \tag{32}$$

Even though the $[\mathbf{C}]$ matrix has dependent rows resulting from a degenerate boundary, the SVD technique can still be employed to find all the true eigenvalues since a sufficient number of constraints is imbedded in the overdeterminate matrix, $[\mathbf{C}]$. As for the true eigenvalues, the rank of the $[\mathbf{C}]$ matrix with dimension $2N \times N$ must as most be $N - 1$ to obtain a nontrivial solution. As for the spurious eigenvalues, the rank must be N to obtain a trivial solution. Based on this criterion, the SVD technique can be

employed to detect the true eigenvalues by checking whether or not the first minimum singular values, σ_1, are zeros. Since discretization creates errors, very small values for σ_1, but not exactly zeros, will be obtained when k is near the critical wave number. In order to avoid the need to determine the threshold for the zero numerically, a value of σ_1 closer to zero must be obtained using a smaller increment near the critical wave number, k. Such a value is confirmed to be a true eigenvalue.

Since Eq. (15) is overdeterminate, we will consider a linear algebra problem with more equations than unknowns:

$$[\mathbf{A}]_{m\times n}\{\mathbf{x}\}_{n\times 1} = \{\mathbf{b}\}_{m\times 1}, \quad m > n \ , \tag{33}$$

where m is the number of equations, n is the number of unknowns and $[\mathbf{A}]$ is the leading matrix which can be decomposed into

$$[\mathbf{A}]_{m\times n} = [\mathbf{U}]_{m\times m}[\mathbf{\Sigma}]_{m\times n}[\mathbf{V}]^*_{n\times n} \ , \tag{34}$$

where $[\mathbf{U}]$ is a left unitary matrix constructed by the left singular vectors, $[\mathbf{\Sigma}]$ is a diagonal matrix which has singular values $\sigma_1, \sigma_2, \ldots,$ and σ_n allocated in a diagonal line as

$$[\mathbf{\Sigma}] = \begin{bmatrix} \sigma_n & \ldots & 0 \\ \vdots & \ddots & \vdots \\ 0 & \ldots & \sigma_1 \\ \vdots & \ddots & \vdots \\ 0 & \ldots & 0 \end{bmatrix}, \quad m > n \ , \tag{35}$$

in which $\sigma_n \geq \sigma_{n-1} \cdots \geq \sigma_1$ and $[\mathbf{V}]^*$ is the complex conjugate transpose of a right unitary matrix constructed by the right singular vectors. As we can see in Eq. (35), there exist at most n nonzero singular values. This means that we can find at most n linear independent equations in the system of equations. If we have p zero singular values ($0 \leq p \leq n$), this means that the rank of the system of equations is equal to $n - p$. However, the singular values may be very close to zero numerically, resulting in rank deficiency. For a general eigenproblem as shown in this paper, the $[\mathbf{C}]$ matrix with dimension $2N \times N$ will have a rank of $N - 1$ for the true eigenvalue with multiplicity 1 and σ_1 is equal to zero theoretically. For true eigenvalues with multiplicity Q, the rank of $[\mathbf{C}]$ will be reduced to $N - Q$ in which $\sigma_1, \sigma_2, \ldots, \sigma_M$ are zeros theoretically. In the case of spurious eigenvalues, the rank for the $[\mathbf{C}]$ matrix is N, and the minimum singular value is not zero.

Determining the eigenvalues of the system of equations has now been transformed into finding the values of k which make the rank of the leading coefficient matrix smaller than N. This means that when $m = 2N, n = N$ and $b_{2N\times 1} = 0$, the eigenvalues will make $p = M$, such that the minimum singular values must be zero or very close to zero.

To find the boundary eigenvector associated with the eigenvalue of multiplicity 1, we can set one of the elements in the boundary eigenvector to be one and then reduce the equations to the form of Eq. (33), where $\mathbf{b}$ is now a nontrivial vector, $m = 2N$ and $n = N - 1$.

Then, the pseudo-inverse matrix, $[\mathbf{A}]^+$ of $[\mathbf{A}]$, is expressed as

$$[\mathbf{A}]^+_{(n-1)\times m} = [\mathbf{V}]_{(n-1)\times(n-1)}[\mathbf{\Sigma}]^+_{(n-1)\times m}[\mathbf{U}]^*_{m\times m} \ , \tag{36}$$

where $\mathbf{\Sigma}^+$ is constructed by taking the transpose of $\mathbf{\Sigma}$ and then replacing the diagonal singular value terms with its inverse, expressed as

$$\mathbf{\Sigma}^+ = \begin{bmatrix} \frac{1}{\sigma_{n-1}} & \ldots & 0 & \ldots & 0 \\ \vdots & \ddots & \vdots & \ddots & \vdots \\ 0 & \ldots & \frac{1}{\sigma_1} & \ldots & 0 \end{bmatrix} \ m > n-1 \ . \tag{37}$$

Since we set a normal quantity in one element of $\{\mathbf{x}\}$ in Eq. (33), none of the singular values for the reduced matrix, $\mathbf{A}_{m\times(n-1)}$, are zeros.

The above-mentioned SVD method has been proved to be equivalent to the least square error solution in determining the unknown vector when the number of equations is larger than the number of unknowns. After introducing the SVD method, we do not need to worry about how to select a specific group of equations such that the rank of the leading coefficient is sufficient to solve for the boundary eigenvector. On the other hand, we can take all the $2N$ equations into account, which apparently causes the rank of the leading coefficient matrix to be equal to $N - 1$ for the true eigenvalue with multiplicity 1. Thus, the boundary eigenvector can be easily found in the sense of the least square error. Another advantage of using SVD is that it can determine the multiplicities for the true eigenvalues by finding the number of singular values which are successively close to zero. A square cavity with eigenvalues of multiplicity 2 will be considered to demonstrate the SVD ability to solve the problem of double roots.

To check the validity of the proposed method, four examples in total will be examined in the following section.

6 Numerical examples

Example 1. Rectangular cavity without partitions subject to the Neumann boundary condition

In this case, an analytical solution is available as follows:

$$\text{eigenvalues: } k_{mn} = \pi\sqrt{\left(\frac{m}{L_x}\right)^2 + \left(\frac{n}{L_y}\right)^2},$$

$$(m, n = 0, 1, 2, \ldots),$$

$$\text{eigenmode: } u_{mn}(x, y) = \cos\left(\frac{m\pi x}{L_x}\right)\cos\left(\frac{n\pi y}{L_y}\right) \ ,$$

where L_x and L_y denote the length and width of the cavity, respectively. In this case, $L_x = 0.236\,m$ and $L_y = 0.112\,m$ for comparison with experiment data obtained by Petyt et al. (1976, 1977). Twenty-four elements are considered in the boundary element mesh. The true eigenvalues contaminated by spurious eigenvalues can be found, as shown in Fig. 1(a) by considering the near zero minimum singular values if only the UT equation is chosen. In a similar

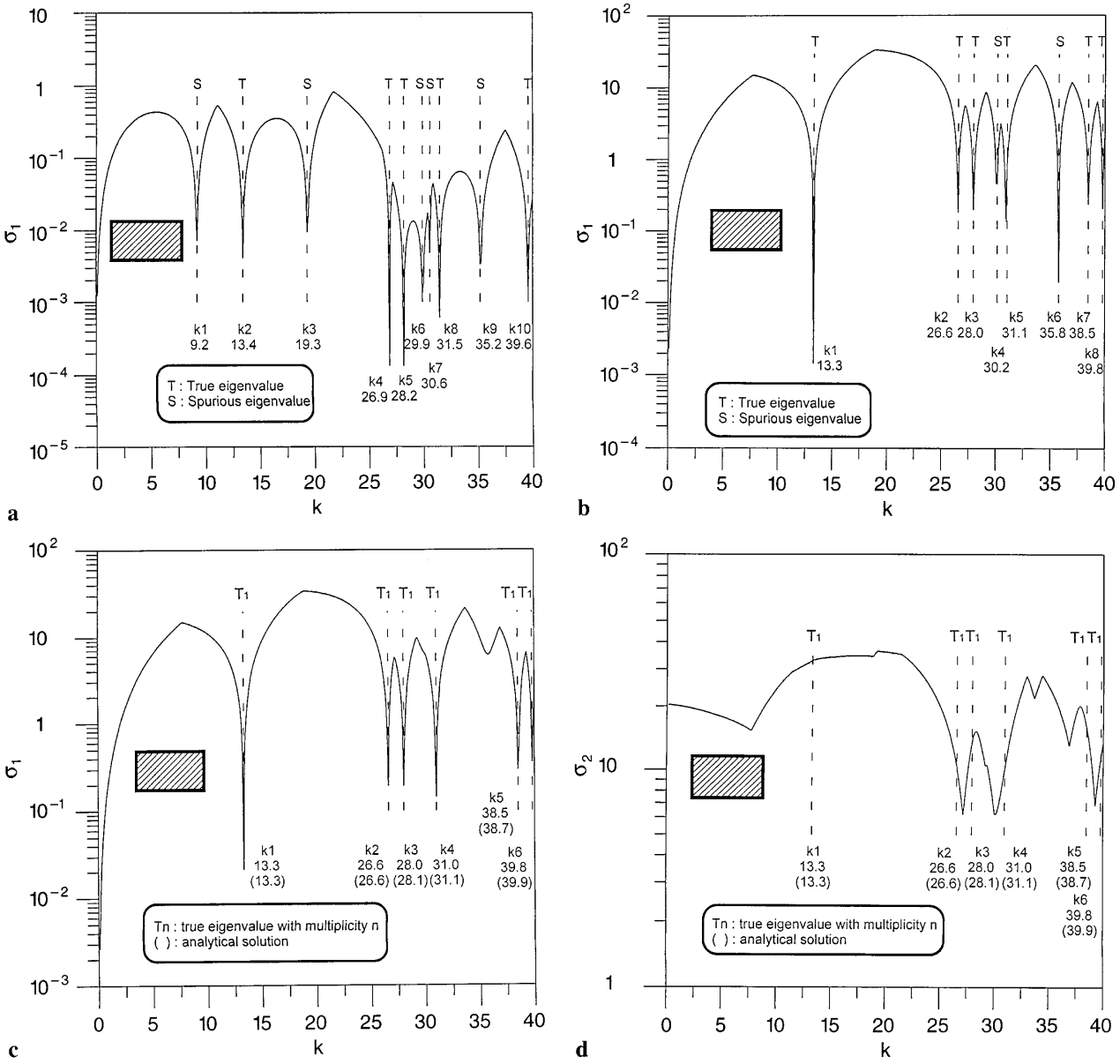

Fig. 1. **a** The first minimum singular values σ_1 versus k using the *UT* equation only for example 1. **b** The first minimum singular values σ_1 versus k using the *LM* equation only for example 1. **c** The first minimum singular values σ_1 versus k using the *UT* and *LM* equations for example 1. **d** The second minimum singular values σ_2 versus k using the *UT* and *LM* equations for example 1

Table 1. The first five critical wave numbers for a rectangular cavity (no partition) using different methods

	Mode 1		Mode 2	Mode 3			Mode 4		Mode 5
Multiplicity	1		1	1			1		1
Analytical solution	13.3		26.6	28.1			31.1		38.7
Complex form (*UT*)	13.3		26.7	28.0			31.1		38.7
Complex form (*LM*)	13.3		26.9	28.0			31.4		38.7
Real part[(a)] (*UT*)	9.2*	13.4	19.3*	26.9	28.2	29.9*	30.6*	31.5	35.2*	39.6
Real part[(b)] (*LM*)		13.3		26.6	28.0		30.2*	31.1	35.8*	38.5
Real part[(c)] (SVD)		13.3		26.6	28.0			31.0		38.5
FEM by ABAQUS (AC2D4)		13.4		26.2	27.7			30.1		36.2
FEM by ABAQUS (AC2D8)		13.5		26.9	28.4			31.4		39.1
Measurement		13.3		28.0	31.0			33.8		41.8

"*a*" denotes data from Fig. 1(a), "*b*" denotes data from Fig. 1(b), "*c*" denotes data from Fig. 1(c), and "*" denotes a spurious root

way, the true eigenvalues contaminated by spurious eigenvalues can be found, as shown in Fig. 1(b), by considering the near zero minimum singular values if only the *LM* equations is chosen. It is interesting to find that no spurious eigenvalues occur in Fig. 1(c) because the *UT* and *LM* equations are combined. This shows that the SVD technique used to filter out spurious eigenvalues can be applied successfully. After obtaining the true eigenvalues, their multiplicities can be determined as given in Fig. 1(d) from the locations where the second minimum singular values approach zero. It is found that no double roots are available in this case. Since no degenerate boundary is present in this case, either the *UT* or *LM* method can be used to solve the problems. In Table 1, two BEM results (obtained using the *UT* and *LM* methods) are shown which have higher accuracy than the ABAQUS solution when compared with the exact solution. Also, the FEM solution obtained by Petyt et al. (1976, 1977) can be obtained using the ABAQUS program. To test the present program, DUALREL, the results were compared with the exact solutions, two ABAQUS results, experimental data obtained by Petyt et al. (1976, 1977) and the results obtained using the complex-valued dual BEM by Chen and Chen (1998) as shown in Table 1. Good agreement is found.

Example 2. Rectangular cavity with a partition of finite thickness subject to the Neumann boundary condition

In this case, a partition with a finite thickness of 0.01 *m* and a height of 0.056 *m* as in Example 1 is considered. The *UT* equation combined with the *LM* method can make the BE model more well-conditioned. Twenty-five elements for the normal boundary and thirteen elements on the partition are adopted in the boundary element mesh. The true eigenvalues contaminated by spurious eigenvalues can be obtained as shown in Fig. 2(a) by considering the near zero minimum singular values if only the *UT* equation is chosen. In a similar way, the true eigenvalues contaminated by spurious eigenvalues can be obtained as shown in Fig. 2(b) by considering the near zero minimum singular values if only the *LM* equation is chosen. No spurious eigenvalues occur in Fig. 2(c) because the *UT* and *LM* equations are combined. This indicates that the SVD technique used to filter out spurious eigenvalues has been applied successfully. After obtaining the true eigenvalues, their multiplicities can be found from the locations where the second minimum singular values approach zero as shown in Fig. 2(d). It is found that no double roots are available in this case. The critical wave numbers are shown in Table 2. FEM results obtained by Petyt et al. (1976, 1977) and obtained using ABAQUS, the complex-valued dual BEM results and the experimental data obtained by Petyt et al. are also compared with the present solutions, and agreement between them is found.

Example 3. Rectangular cavity with a partition of zero thickness (the *UT* method combined with the *LM* equation)

When the thickness of the partition in Example 2 becomes zero, the dual formulation for the real-part BEM can be employed to solve the problem. Twenty-five elements for the normal boundary and twelve elements on the partition are adopted in the boundary element mesh. Since two alternatives, the *UT* or *LM* equation, can be chosen for collocating on the outer (normal) boundary, two results from the *UT* and *LM* methods can be obtained. Fig. 3(a) shows the minimum singular value versus k. The true eigenvalues contaminated by spurious eigenvalues can be obtained as shown in Fig. 3(a) by considering the near zero minimum singular values if only the *UT* equation, combined with the *LM* equation by collocating the point on the partition, is chosen. In a similar way, the true eigenvalues contaminated by spurious eigenvalues can be obtained as shown in Fig. 3(b) by considering the near zero minimum singular values if only the *LM* equation, combined with the *UT* equation by collocating the point on the partition, is chosen. No spurious eigenvalues occur in Fig. 3(c) because the *UT* and *LM* equations are combined together. This shows that the SVD technique has been applied successfully to filter out spurious eigenvalues. After obtaining the true eigenvalues, their multiplicities can be determined as shown in Fig. 3(d) from the locations where the second minimum singular values approach zero. It is found that no double roots are available in this case. The critical wave numbers are shown in Table 3. The FEM results obtained by Petyt et al. (1976, 1977) and those obtained using ABAQUS, the complex-valued dual BEM results obtained by Chen and Chen (1998) and the experimental data obtained by Petyt et al. (1976, 1977) have also been compared with the present solutions, and agreement has been found between the numerical results and experimental data.

Example 4 with degenerate eigenvalues will next be considered. The multiplicity is two for the degenerate eigenvalues. In the direct search method using the half method or false position method, the degenerate eigenvalues may be lost since no zero crossing for a determinant can be found numerically. Therefore, use of the SVD technique is strongly suggested in order to filter out the spurious eigenvalues and to determine the multiplicity for the true eigenvalues.

Example 4. A square cavity with a radius of 1 *m* subject to the Neumann boundary condition

In this case, an analytical solution is available as follows:

$$\text{eigenequation } J'_m(k_{mn}) = 0, m, n = 1, 2, 3 \ldots;$$

$$\text{eigenmode : } u(r, \theta) = J_m(k_{mn} r) e^{im\theta} \quad .$$

Eighty elements are adopted in the boundary element mesh. Since two alternatives, the *UT* or *LM* equation, can be chosen for collocating on the boundary, two results from the *UT* and *LM* methods can be obtained. Fig 4(a) shows the minimum singular value versus k. The true eigenvalues contaminated by spurious eigenvalues can be obtained as shown in Fig. 4(a) by considering the near zero minimum singular values if only the *UT* equation is chosen. In a similar way, the true eigenvalues contaminated by spurious eigenvalues can be obtained as shown in Fig. 4(b) by considering the near zero minimum singular values if only the *LM* is chosen. It is interesting to find that no spurious eigenvalues occur as shown in

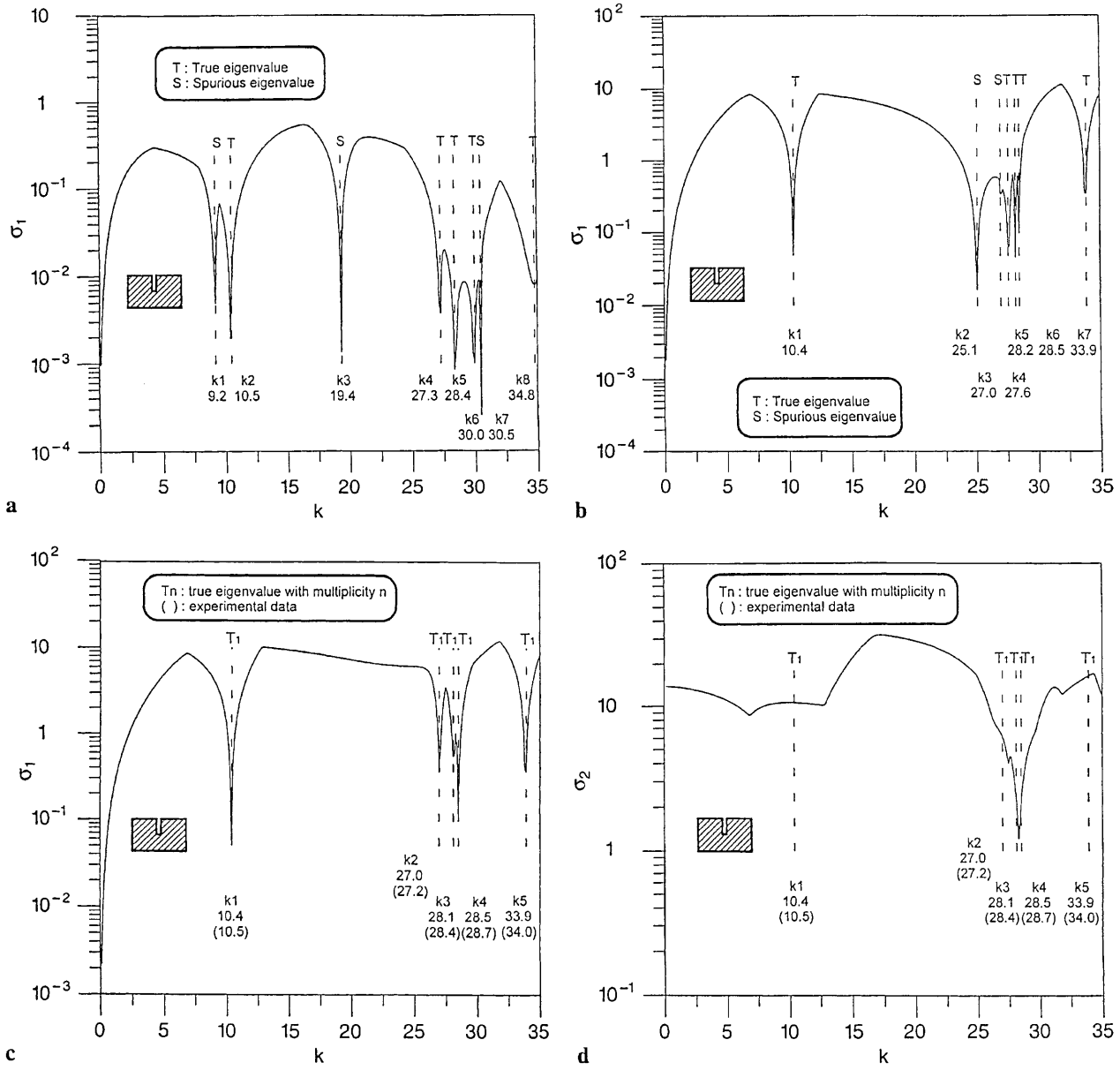

Fig. 2. **a** The first minimum singular values σ_1 versus k using the *UT* equation only for example 2. **b** The first minimum singular values σ_1 versus k using the *LM* equation only for example 2. **c** The first minimum singular values σ_1 versus k using the *UT* and *LM* equations for example 2. **d** The second minimum singular values σ_2 versus k using the *UT* and *LM* equations for example 2

Table 2. The first five critical wave numbers for a rectangular cavity with a finite thickness partition using different methods

	Mode 1			Mode 2	Mode 3	Mode 4		Mode 5
Multiplicity	1			1	1	1		1
Complex form (*UT*)	10.9			26.7	28.0	28.6		34.0
Complex form (*LM*)	10.9			26.7	28.0	28.4		34.0
Real part$^{(a)}$ (*UT*)	9.2*	10.5	19.4*	27.3	28.4	30.0	30.5*	34.8
Real part$^{(b)}$ (*LM*)	10.4	25.1*	27.0*	27.6	28.2	28.5		33.9
Real part$^{(c)}$(SVD)	10.4			27.0	28.1	28.5		33.9
FEM by ABAQUS (AC2D4)	10.9			26.7	27.8	28.2		33.0
FEM by ABAQUS (AC2D8)	10.7			27.4	28.5	28.9		34.3
FEM by Petyt	10.7			26.8	28.6	29.8		34.4
Measurement	10.5			27.2	28.4	28.7		34.0

"*a*" denotes data from Fig. 2(a), "*b*" denotes from Fig. 2(b), "*c*" denotes data from Fig. 2(c), and "*" denotes a spurious root

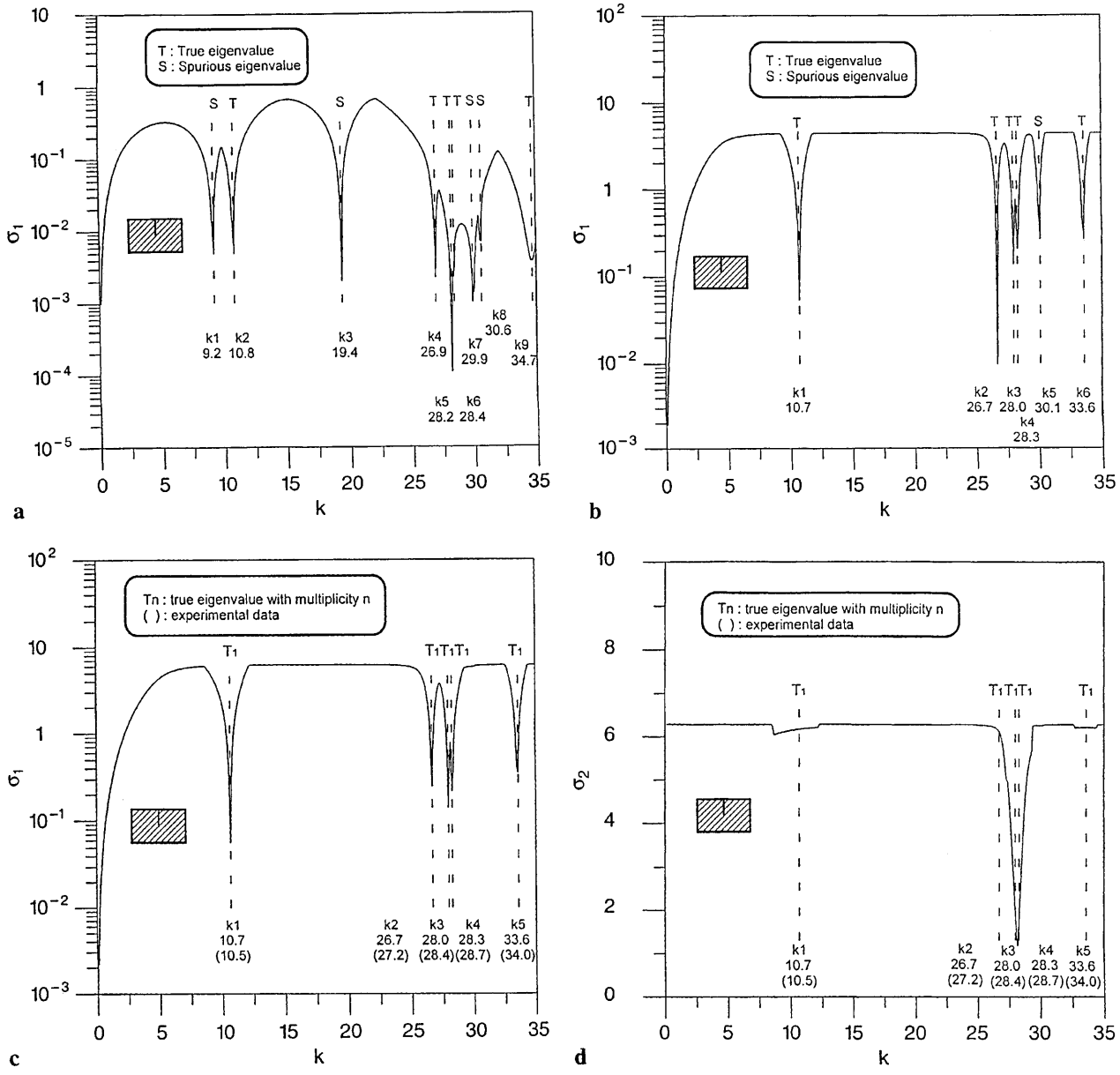

Fig. 3 **a** The first minimum singular values σ_1 versus k using the *UT* equation only for example 3. **b** The first minimum singular values σ_1 versus k using the *LM* equation only for example 3. **c** The first minimum singular values σ_1 versus k using the *UT* and *LM* equations for example 3. **d** The second minimum singular values σ_2 versus k using *UT* and *LM* equations for example 3

Table 3. The first five critical wave numbers for a rectangular cavity with a zero thickness partition using different methods

	Mode 1		Mode2	Mode3	Mode4			Mode 5
Multiplicity	1		1	1	1			1
Complex form (*UT* + *LM*)	10.8		26.6	28.1	28.4			33.6
Complex form (*LM* + *UT*)	10.8		26.6	28.1	28.4			33.6
Real part[(a)] (*UT*)	9.2*	10.8	19.4*	26.9	28.2	28.4	29.9*	30.6*	34.7
Real part[(b)] (*LM*)		10.7		26.7	28.0	28.3	30.1*	33.6*	35.9
Real part[(c)] (SVD)		10.7		26.7	28.0	28.3			33.6
FEM by ABAQUS (AC2D4)		11.4		26.3	27.7	28.2			32.9
FEM by ABAQUS (AC2D8)		11.2		26.9	28.4	28.9			34.2
FEM by Petyt		10.9		27.3	28.5	29.0			34.4
Measurement		10.5		27.2	28.4	28.7			34.0

"*a*" denotes data from Fig. 3(a), "*b*" denotes data from Fig. 3(b), "*c*" denotes data from Fig. 3(b), and "*" denotes a spurious root

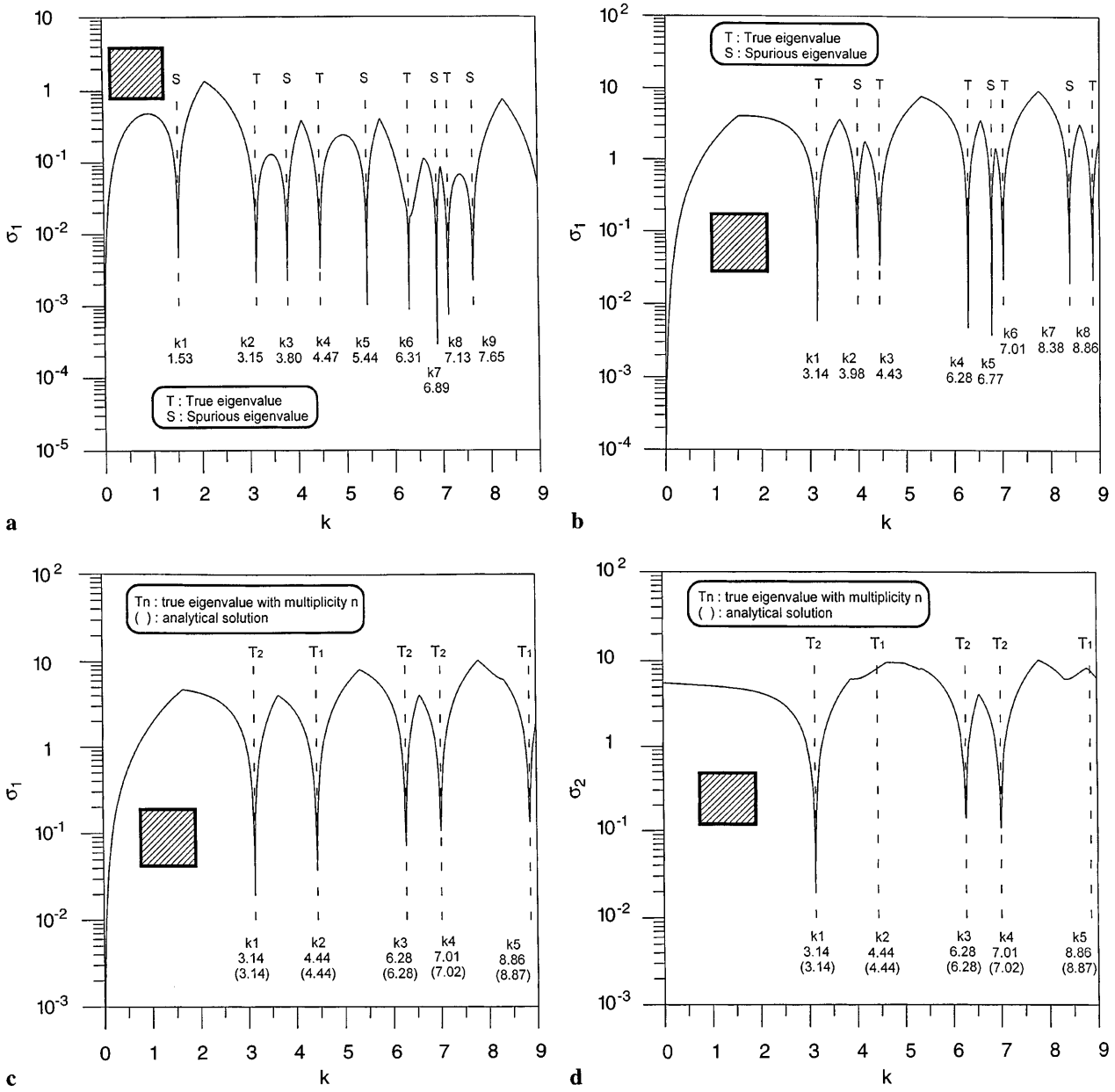

Fig. 4 **a** The first minimum singular values σ_1 versus k using the *UT* equation only for example 4. **b** The first minimum singular values σ_1 versus k using the *LM* equation only for example 4. **c** The first minimum singular values σ_1 versus k using the *UT* and *LM* equations for example 4. **d** The second minimum singular values σ_2 versus k using the *UT* and *LM* equations for example 4

Table 4. The first five critical wave numbers for a square cavity (Neumann type) using different methods

	Mode 1		Mode 2		Mode 3		Mode 4		Mode 5
Multiplicity	2		1		2		2		1
Analytical Solution	3.14		4.44		6.28		7.02		8.87
Complex form (*UT*)	3.14		4.44		6.32		7.02		8.89
Complex form (*LM*)	3.14		4.44		6.32		7.02		8.89
FEM by ABAQUS	3.18		4.49		6.36		7.10		8.99
Real part$^{(a)}$ (*UT*) 1.53*	3.15	3.80*	4.47	5.44*	6.31	6.89*	7.13	7.65*	9.13
Real part$^{(b)}$ (*LM*)	3.14	3.98*	4.43		6.28	6.77*	7.01	8.38*	8.86
Real part$^{(c)}$ (SVD)	3.14		4.44		6.28		7.01		8.86

"*a*" denotes data from Fig. 4(a), "*b*" denotes data from Fig. 4(b), "*c*" denotes data from Fig. 4(c), and "*" denotes a spurious root

Fig. 4(c) when the *UT* and *LM* equations are combined. After obtaining the true eigenvalues, their multiplicities can be determined as shown in Fig. 4(d) from the locations where the second minimum singular values approach zero. It is found that double roots are obtained in this case. Since no triple roots are available, the plot of σ_3

versus k is not provided. The critical wave numbers are shown in Table 4. Good agreement among the different methods, the complex-valued BEM, the analytical solution and the present method, have been obtained.

7 Conclusions

The real-part dual BEM in conjunction with the SVD technique has been applied to determine the critical wave numbers of a cavity with or without a thin partition, and with or without multiple roots. The nonuniqueness of the solution due to the zero thickness partition and spurious eigenvalues, which are encountered when using the real-part *UT* or *LM* equation alone, can be treated at the same time. A general purpose program, DUALREL, has been developed to determine the eigenvalues of an arbitrary cavity with or without a partition, and with or without double roots. The spurious eigenvalues in the real-part dual BEM have been successfully filtered out, and the multiplicity for the true eigenvalues for the square cavity have been determined by using the SVD technique. Numerical results show that the present method can predict the eigenvalues more efficiently than can the FEM. In addition, the numerical results match the experiment data well.

References

Chang JR, Yeih W, Chen JT (1999) Determination of the natural frequencies and natural modes of a rod using the dual BEM in conjunction with the superelement concept. Comp. Mech., Accepted

Chen JT (1998) Recent development of dual BEM in acoustic problems, Keynote lecture. Proceedings of the 4th World Congress on Computational Mechanics, E. Onate and S.R. Idelsohn (eds), Argentina, p. 106

Chen JT, Chen KH (1998) Dual integral formulation for determining the acoustic modes of a two-dimensional cavity with a degenerate boundary. Eng. Anal. Bound. Ele. 21:105–116

Chen JT, Chen KH, Chyuan SW (1999) Numerical experiments for acoustic modes of a square cavity using dual BEM. Appl. Acou. 57:293–325

Chen JT, Hong H-K (1992) Boundary element method, New World Press 2nd Ed., Taipei, Taiwan (in Chinese)

Chen JT, Hong H-K (1999) Review of dual integral representations with emphasis on hypersingular integrals and divergent series. Transations of ASME, Applied Mechanics Reviews 52:17–33

Chen JT, Huang CX, Wong FC (1998) Analysis and experiment for acoustic modes of a cavity containing an incomplete partition, Proceedings of the Fourth National Conference on Structural Engineering, 1:349–356

Chen JT, Wong FC (1997) Analytical derivations for one-dimensional eigenproblems using dual BEM and MRM. Eng. Anal. Bound. Ele. 20:25–33

Chen JT, Wong FC (1998) Dual formulation of multiple reciprocity method for the acoustic mode of a cavity with a thin partition. J. of Sound and Vibration 217:75–95

De Mey G (1977) A simplified integral equation method for the calculation of the eigenvalues of Helmholtz equation. Int. J. Num. Meth. Engng 11:1340–1342

Gloub GH, Van Loan CF (1989) Matrix Computations, 2nd edition, The Johns Hopkins University Press, Baltimore

Kamiya N, Andoh E, Nogae K (1996) A new complex-valued formulation and eigenvalue analysis of the Helmholtz equation by boundary element method. Advances in Eng. Software 26:219–227

Liou DY, Chen JT, Chen KH (1999) A New Method for Determining the Acoustic Modes of a Two-dimensional Sound Field. Journal of the Chinese Institute of Civil and Hydraulic Engineering Accepted (in Chinese)

MSC/ABAQUS User Manual. MSC Version 5.5, 1996

Nowak AJ, Neves AC, eds. (1994) Multiple Reciprocity Boundary Element Method, Sonthampton: Comp. Mech. Publ

Petyt M, Lea J, Koopmann GH (1976) A finite element method for determining the acoustic modes of irregular shapes cavities. J. Sound and Vibration 45:495–502

Petyt M, Koopmann GH, Pinnigton RJ (1997) Acoustic modes of rectangular cavity with a rigid incomplete partition. J. Sound and Vibration 53:71–82

Press WT, Teukosky SA, Vetterling WT, Flannery BP (1992) Numerical Recipes in FORTRAN, 2nd edition, Cambridge University Press, New York

Yeih W, Chang JR, Chang CM, Chen JT (1999) Applications of dual MRM for determining the natural frequencies and natural modes of a rod using the singular value decomposition method. Advances in Engineering Software, Accepted

Yeih W, Chen JT, Chang CM (1999) Applications of dual MRM for determining the natural frequencies and natural modes of an Euler-Bernoulli beam using the singular value decomposition method. Engineering Analysis with Boundary Elements. 23:339–360

Yeih W, Chen JT, Chen KH, Wong FC (1997) A study on the multiple reciprocity method and complex-valued formulation for the Helmholtz equation. Advances in Eng. Software 29:1–6